Meetings in Physics at University of Sofia, vol. 5
ed. A. Proykova, Heron Press, Sofia, 2004

MECHANICALLY INDUCED DEFECTS IN SINGLE-WALL CARBON NANOTUBES

H. Iliev and A. Proykova

Authors address: Department of Atomic Physics, Faculty of Physics, Sofia University, Sofia-1126, 5 J. Bourchier Blvd.

Abstract. We use the Molecular Dynamics method with a modified Brenner-Tersoff potential to study how various defect distributions influence the tensile strength of single-wall carbon nanotubes. We model defect formation under external mechanical loads (stress and stretch). The stability of the tubes and the reversibility of the process are also investigated.

Nomenclature

i	atom index
$\mathbf{r}_i$	coordinate
m_i	mass
E_b	structure binding energy
$\mathbf{F}_i$	force over i-th atom
$\mathbf{F}_{ext}$	external force
$\mathbf{a}^i$	i-th unit chiral vector

1. Introduction

A single-wall carbon nanotube is a rolled-up single graphite sheet (graphene) so as to make a cylinder, Fig.1. The vector $\mathbf{C}_h = n\mathbf{a}^1 + m\mathbf{a}^2 \equiv (n, m)$, where n and m are integers, is called *chiral vector*. It determines the tube curvature and hence the electric conductivity.

The carbon nanotubes were discovered in 1991 by the Japanese electron microscopist Sumio Iijima [1] who was studying the material deposited on the cathode during the arc-evaporation synthesis of fullerenes. Generally, tubes are conductors if $|n - m| \equiv 3k$ where k is a non-negative integer, and otherwise semiconductors. Tubes with extremely small radius violate that rule because of the bigger overlap of the π-orbitals due to the curvature [2]. The one-dimensional nature of conduction within nanotubes [3] makes it possible to explore and verify the quantum physics theory. From a practical point of view, CNT bring advances in nanodevice design.

Recently, an interesting topic has been how mechanical deformations of a SWCNT affects its electronic property [4, 5, 6, 7, 8]. Previous studies [7, 8] show that in many cases, a local deformation can not drive a metal-to-semiconductor transition (MST) in armchair (n,n) SWNTs. At the same time, a recent work [9] indicates that a MST can be achieved by a radial deformation along the holistic armchair SWNTs. Measurements [10] of the temperature dependent *dc* and *ac* electrical resistance of single-wall-nanotube ropes show that they are metallic at high temperatures and exhibit a crossover to nonmetallic behaviour at a low temperature. The transition temperature is different for the different samples and is sensitive to mechanical handling. It has been suggested that the origin of the low-temperature nonmetallic behaviour is 1D localization and motivated another measurements [11] to provide experimental confirmation of band structure calculations for SWCNT. Hone et al have studied the temperature dependence of the thermoelectric power (TEP) because its sign indicates the sign of the dominant current carrier, thus giving information about the type of conduction: TEP is linear in T for metals and

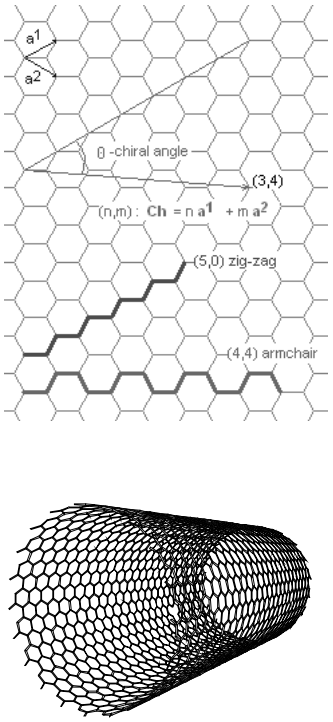

Figure 1. The rolled-up graphite sheet makes a tube

changes as (1/T) for a true-gap semiconductor. Hone et al conclude from their experiment that a SWCNT is metal-like $T \approx 0$, while ropes might mimic semiconducting behaviour due to charge transfer between tubes with different defects.

The goal of the present paper is to demonstrate how various defect distributions affect SWCNT's mechanical stability and, through it, the electrical properties of SWCNTs. Our toy system is a zigzag (10,0) tube containing 2000 carbon atoms. Previous molecular dynamics simulations predict that ideal SWCNTs should possess extremely high tensile strengths. The strain at tensile failure has been predicted to be $\sim 30\%$ in [12] and $\sim 45\%$ in [13]. The two papers use different parameterization of the interacting (Brenner-Tersoff) potential. This potential belongs to the category of potentials called *molecular mechanics force fields* that are used for systems where the covalent bonds never break. Comparing the results from [12, 13] to the experimental findings [14]: the failure is between 2% and 15%, we should agree that either the Brenner potential is too robust or the carbon nanotubes are defected. There are results for softer potentials in the literature. For example, the work [15] implements a modified Morse potential with parameters adjusted so that it coincides with the Brenner potential for strains below 10%.

2. Simulation technique

We employ classical Molecular Dynamics [16] to study defected tube response to an external field. The equations of motion are integrated numerically in their Newtonian form:

$$m_i \ddot{\mathbf{r}}_i(t) = \mathbf{F}_i(t) = -\nabla_{\mathbf{r}_i} E_b \tag{1}$$

with E_b being the binding energy of the system. We use a simplified form of the Brenner-Tersoff potential:

$$E_b = \sum_i \sum_{j(>i)} \left[V_R(r_{ij}) - \bar{B}_{ij} V_A(r_{ij}) \right], \tag{2}$$

i and j run over all atomic sites; r_{ij} is the distance between atoms i and j. V_R is the repulsive term and has the form:

$$V_R(r_{ij}) = f_{ij}(r_{ij}) \frac{D_{ij}^{(e)}}{S_{ij} - 1} e^{-\sqrt{2S_{ij}}\beta_{ij}\left(r_{ij} - R_{ij}^{(e)}\right)} \tag{3}$$

while V_A is the attractive term and has a similar form:

$$V_A(r_{ij}) = f_{ij}(r_{ij}) \frac{D_{ij}^{(e)} S_{ij}}{S_{ij} - 1} e^{-\sqrt{2/S_{ij}}\beta_{ij}\left(r_{ij} - R_{ij}^{(e)}\right)} \tag{4}$$

f_{ij} is a cut-off function which restricts the pair interaction to nearest neighbors only:

$$f_{ij}(r) = \begin{cases} 1 & r < R_{ij}^{(1)}, \\ \frac{1}{2}\left[1 + \cos\frac{\pi\left(r - R_{ij}^{(1)}\right)}{R_{ij}^{(2)} - R_{ij}^{(1)}}\right] & R_{ij}^{(1)} < r < R_{ij}^{(2)} \\ 0 & R_{ij}^{(2)} < r \end{cases} \tag{5}$$

$\bar{B}_{ij} = (B_{ij} + B_{ji})/2$ is an empirical bond-order function with each of the averaged terms in the form:

$$B_{ij} = \left[1 + \sum_{k(\neq i,j)} G_i(\phi_{ijk}) f_{ik}(r_{ik}) \times e^{\alpha_{ijk}\left[\left(r_{ij} - R_{ij}^{(e)}\right) - \left(r_{ik} - R_{ik}^{(e)}\right)\right]}\right]^{-\delta_i} \tag{6}$$

Parameter	Value	Parameter	Value
$R_{ij}^{(e)}$	1.39 Å	$R_{ij}^{(1)}$	1.7 Å
$D_{ij}^{(e)}$	6.0 eV	$R_{ij}^{(2)}$	2.0 Å
β_{ij}	2.1 Å^{-1}	a_0	0.00020813
S_{ij}	1.22	c_0^2	330^2
δ_{ij}	0.5	d_0^2	3.5^2
α	0.0		

Table .1. Potential parameters used in simulations

In presence of an external force field $\mathbf{F}_{ext}(\mathbf{r})$ (stress or twist), the Newtonian equations become:

$$m_i \ddot{\mathbf{r}}_i(t) = -\nabla_{\mathbf{r}_i} E_b + \mathbf{F}_{ext}(t) \tag{7}$$

Integration is performed with the velocity Verlet algorithm [16], which advances in time the particle positions and velocities as follows:

$$\left|\begin{array}{l} \mathbf{r}_i(t+dt) = \mathbf{r}_i(t) + dt\mathbf{v}_i(t) + (1/2m)dt^2\mathbf{F}_i(t) \\ \mathbf{v}_i(t+dt) = \mathbf{v}_i(t) + (1/2m)dt[\mathbf{F}_i(t) + \mathbf{F}_i(t+dt)] \end{array}\right. \tag{8}$$

where $\mathbf{F}_i = -\nabla_{\mathbf{r}_i} E_b + \mathbf{F}_{ext}(\mathbf{r}_i)$ is the force, acting on i-th atom. The cell linked-list method, combined with the Verlet neighboring list [16] have been used to speed-up the calculations.

The external load is simulated by enforcing a constant change in the position of the edge atoms $\{\mathbf{r}_i\}$ in the form:

$$\mathbf{r}_i(t+dt) = \mathcal{U}(z_i)\mathbf{r}_i(t) \tag{9}$$

where $\mathcal{U}(z_i)$ is the evolution operator of the edge atoms that equals $\mathcal{T}(\pm\delta\mathbf{r})$ (translation) in the case of stress or $\mathcal{R}(\pm\delta\phi)$ (rotation) in the case of stretch where the $(+)$ sign is for atoms with $z_i > 0$ and the $(-)$ sign is for atoms with $z_i < 0$. The positions and velocities of the remaining atoms are computed using the velocity Verlet scheme depicted above.

In this work we focus on tubes with missing atoms. In experiments performed with the help of the transmission electron microscopy it is possible for single atoms to be ejected by impact [17]. For a given percentage of vacancies$(1\%, 5\%, 10\%)$ we randomly choose the positions of atoms to be ejected. In practice, we break the bonds between the atom chosen and its nearest neighbours. Then we apply an external force to the defected tube (a tube with a certain amount of defects) and monitor the energy accumulated and the time necessary to cause fracture as functions of the defect distributions. The interpretation of fracture simulations by atomistic models is not strait-forward because the reconstruction of bonds, after an atom is ejected, is not considered.

3. Results

Acknowledgments

This research was supported by the Bulgarian Ministry of Education and Science under grant F-3/2003. H. Iliev acknowledges the support from the European Commission through grant number HPRI-CT-1999-00026 (the TRACS programme at EPCC, University of Edinburgh).

Reference

[1] S. Iijima (1991)*Nature* (London) **354**, 56.

[2] L. Yang, M. Anantram, J. Han, J. P. Lu (1999) *Phys. Rev. B* **60(19)**, 13874

[3] J.W.G. Wilder, L.C. Venema, A.G. Rinzler, Smalley, C. Dekker (1998) *Nature* (London) 59.

[4] T.W. Tombler, C. Zhou, L. Alexseyev, J. Ko Dai, L. Liu, C.S. Jayanthi, M. Tang, S. Wu (*Nature* (London) **405**, 769.

[5] E.D. Minot, Y. Yaish, V. Sazonova, J.Y. Pa Brink, P.L. McEuen (2003) *Phys. Rev. Let* 156401.

[6] J. Cao, Q. Wang, H. Dai (2003) *Phys. Rev.* **90**, 157601.

[7] A. Maiti, A. Svizhenko, M.P. Anantram (*Phys. Rev.Lett.* **88**, 126805.

[8] M.B. Nardelli, J. Bernholc (1999) *Phys. Rev.* R16338.

[9] J.Q. Lu, J. Wu, W. Duan, F. Liu, B.F. Zhu Gu (2003)*Phys. Rev. Lett.***90**, 156601.

[10] J.E. Fischer, H. Dai, A. Thess, R. Lee, N.M. jani, D.L. Dehaas, R.E. Smalley (1997)*Phys.* **55**, R4921.

[11] J. Hone, I. Ellwood, M. Muno, Ari Mizel, M L. Cohen, A. Zettl (1998) *Phys. Rev. Lett* **80**,

[12] M.P. Campbell, C.J. Barbec, J. Be (1997)*Comput. Mat.Sci.***8**, 341.

[13] A. Proykova, H. Iliev (2004) in *SIMS2004*, p 279, eds. Brian Elmegaard, Jon Sporring, I Erleben, Kim Sorensen (ISBN 87-7475-316 9)

[14] M.F. Yu, O. Louire, M.J. Dyer, K. Moloni, Kelly, R.S. Ruoff (2000) *Science* **287**, 637.

[15] T. Belytschko, S.P. Xiao, G.C. Schatz, and Ruoff (2002) *Phys. Rev. B***65**, 235430.

[16] M. Allen, D. Tildesley (1986) *Computer simu of liquids*, Oxford Science Publications

[17] F. Banhart (1999) *Rep. Prog. Phys.* **62**,1181.

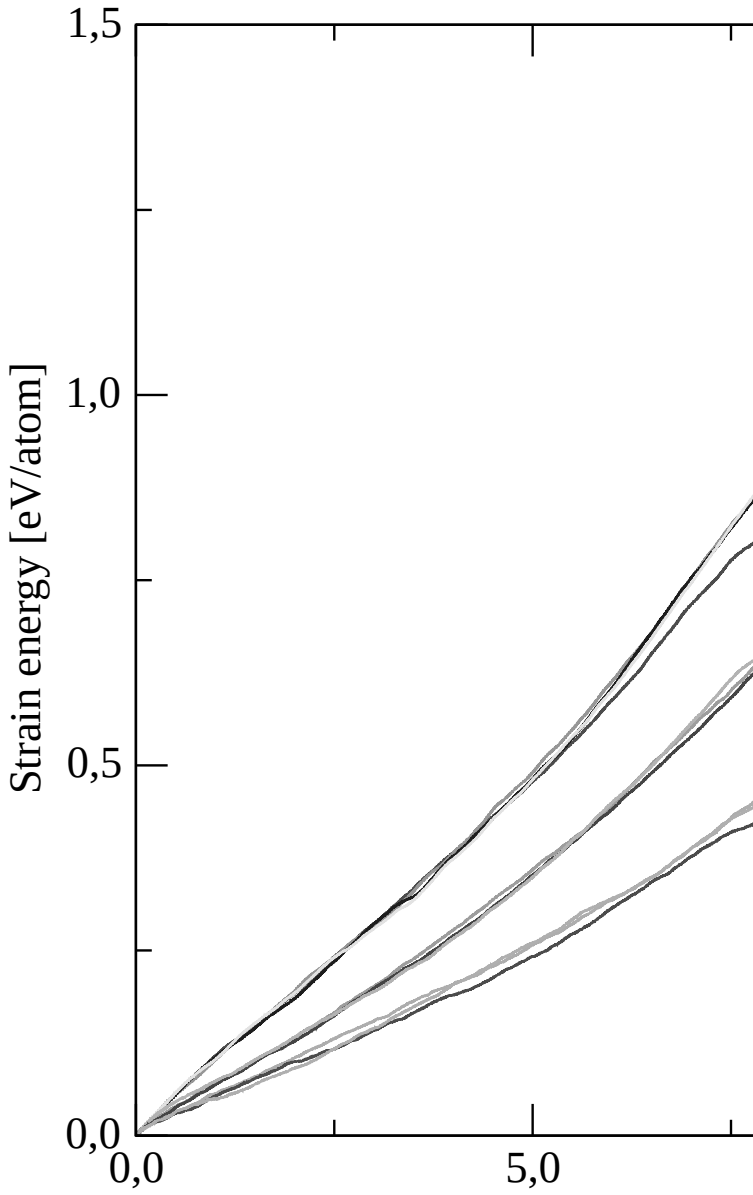

Figure 2. The effect of defect concentration on the strain energy per atom in a (10,0) SWCNT with 2000 atoms. For every concentration we present sevral curves correponding to different defect distributions. We use a random generator to distribute the defects.